CORE
Metadata, citation and similar papers at core.ac.uk
Provided by Ulster University's Research Portal

Fire Behaviour of Gypsum Plasterboards Enhanced with Phase Change Materials: A CFD Study

Dionysios I. Kolaitis; Eleni K. Asimakopoulou; Maria A. Founti*

Laboratory of Heterogeneous Mixtures and Combustion Systems, Thermal Engineering Section,
School of Mechanical Engineering, National Technical University of Athens
9, Heroon Polytechniou St., Polytechnioupoli Zografou, Athens 15780, Greece.
**e-mail: dkol@central.ntua.gr, Tel.: +30-210-7724002, Fax: +30-210-7723527*

ABSTRACT

Phase Change Materials (PCM) can be used for thermal energy storage, aiming to enhance building energy efficiency. Recently, gypsum plasterboards with incorporated paraffin-based PCM blends have become commercially available. In the event of a fire, building elements are exposed to substantially high temperatures; in this case, paraffins, exhibiting relatively low boiling points, may evaporate and, escaping through the gypsum plasterboard's porous structure, emerge to the fire region, where they may ignite, thus adversely affecting the fire resistance characteristics of the building. Aiming to investigate the occurring physical phenomena, a CFD code is used to simulate a model room exposed to fire conditions, which is alternatively assumed to be clad with either "plain" or "PCM-enriched" gypsum plasterboards. The impact of PCM addition to the overall fire behaviour of gypsum plasterboards is investigated by utilizing predictions of the temporal evolution of wall surface temperature, gas mixture velocity and temperature. Differential Scanning Calorimetry (DSC) and Thermo Gravimetric Analysis (TGA) tests are performed to determine the main thermo-physical properties of PCM-enriched gypsum plasterboards. Numerical results show that PCM may indeed adversely affect the fire resistance characteristics of a gypsum plasterboard clad building.

1 INTRODUCTION

Uncontrollable fires in buildings represent a significant part of fire-related fatalities. Investigation of the commonly used building materials' fire behaviour is of primary interest since the developed thermal environment and the production of toxic gases are associated with a large range of hazards to human life and properties. In building fires, the confined space controls the ventilation conditions and fuel load affect the developing thermal field, thus influencing the thermal exposure of structural elements [1, 2]. Experimental and numerical methods can be utilized for the understanding of the dynamics of a fire incident, the estimation of structural fire resistance and the quantification of its overall impact on buildings and people; both approaches are equally valuable to analyse the occurring physical and chemical phenomena. In the context of numerical simulation, the growing processing power of modern computers has resulted in the increasing utilization of Computational Fluid Dynamics (CFD) tools (also described as "field models") in all aspects of fire safety

engineering, thus establishing their precedence over the "zone models", widely used in the past [3, 4, 5].

Phase Change Materials (PCM) are used in a wide range of applications; they can be incorporated in building materials, aiming to increase the thermal mass storage capacity of a building [6]. This innovative technique takes advantage of the latent heat of the PCM during the solid-to-liquid phase change to reduce the indoor temperature fluctuations and the heat losses/gains between the building and the environment [7]. PCM can be incorporated in concrete, gypsum plasterboards, plaster and other building materials using various impregnation methods. Traditional methods for incorporating PCM, such as direct incorporation, immersion and macro-encapsulation, have fallen into disuse due to leakage problems, incompatibility, tendency of solidification at the edges, poor thermal conductivity and complicated integration to the building materials [8, 9]. Nowadays, micro-encapsulated PCM are commonly used as an easier and more economic way of incorporation into construction materials. Micro-encapsulation of the PCM prior to incorporation to the building material is favoured in commercial applications [10, 11]. PCM particles enclosed in thin sealed polymer spherical-like capsules, which range in size from 1 μm to 300 μm, can maintain their shape and prevent leakage during the phase change process [12]. In commonly used PCM, the solid-liquid phase change occurs in the typical temperature range found indoors (20-26oC), which is favourable for building energy consumption purposes. However, in a fire event, building materials may be exposed to substantially higher temperatures, that may reach 800^{o}C; in this case, there is always the possibility for leakage, which would render PCM vapours directly exposed to the fire environment [13, 14]. In such intense heating conditions, paraffin-based PCM are expected to evaporate, since the boiling point of typical paraffins lies below 350^{o}C. If the PCM encapsulation shell is broken, due to the high temperature environment, the produced paraffin vapours will be released to the porous structure of the gypsum plasterboard and, through mass diffusion processes, will emerge to the main combustion region. In this case, paraffin vapours are expected to ignite, thus adversely affecting the building's fire resistance characteristics [15]. The impact of this effect is investigated in the current study, using a CFD tool to simulate a model room exposed to fire conditions.

2 NUMERICAL SIMULATION

2.1 Description of the Geometry

In order to investigate the effect of PCM addition to the fire behaviour of gypsum plasterboards, a standard "Room Corner Test" (ISO 9705) geometry is used. The main room dimensions are 2.4 m x 3.6 m x 2.4 m; a 0.8 m x 2.0 m open door is located on a rectangular side wall (Figure 1). Detailed measurements obtained by the NIST Large Fire Research Laboratory are used for validation purposes [16]; available data include the temporal evolution of gas temperature and species concentrations (e.g. O_2, CO, CO_2) in two (F-front and R-rear) positions located at the upper layer of the compartment (Figure 1). The fire source used in this study was assumed to be a rectangular (1.0 m x 1.0 m) burner, located at the geometrical centre of the room (Figure 1), which is fed with n-heptane, exhibiting a constant

2070 kW heat release rate, in accordance to the last “step” of the experimental over-ventilated fire test case (ISOHept4) presented in [16].

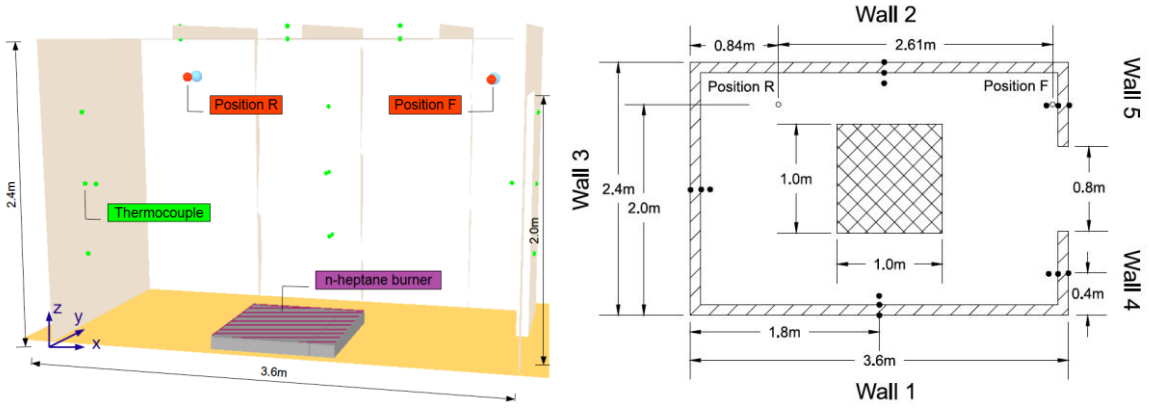

Figure 1. General configuration (left) and top section (right) of the model room and the measuring locations.

2.2 Description of the CFD Code

The Fire Dynamic Simulator (FDS, Version 5.5.3), developed by NIST [17], is used to perform the compartment pool fire simulations. The FDS code is a CFD tool capable of studying fundamental fire dynamics and combustion, aimed at solving practical fire problems in fire protection engineering. A form of the Navier-Stokes equations appropriate for low-speed, thermally driven flows, emphasizing on smoke production and heat transfer from fires, are numerically solved. The partial derivatives of the conservation equations of mass, momentum and energy are approximated as finite differences and the solution is updated in time on a three-dimensional, Cartesian grid. Scalar quantities are assigned in the centre of each grid cell and vector quantities are assigned at the respective cell faces. The core algorithm is a semi-implicit (explicit in velocity and implicit in pressure) predictor-corrector scheme that is second order accurate in space and time by using central differences. In the first predictor step, FDS computes a rough approximation of the thermodynamic quantities that are necessary in order to be able to proceed to the next time step. At the next time step, the velocity is estimated using a new pressure term from the solution of the Poisson equation. Based on this estimation of velocity, a corrector step modifies the thermodynamic quantities and computes the corrected velocity using a recomputed pressure term. The numerical scheme in FDS requires the solution of the Poisson equation for the computation of the pressure twice within a time iteration.

The turbulent viscosity are modelled using the Large Eddy Simulation (LES) approach for length scales smaller than those that are explicitly resolved on the numerical grid [18]. A filtration procedure is employed using the characteristic grid cell length as the filter width. Averaging is only performed for turbulent fluctuations exhibiting length scales smaller than the filter width and a subgrid turbulence model is used for the small-scale turbulent viscosity. The subgrid-scale turbulence is simulated using the Smagorinsky model, utilizing a Smagorinsky constant (C_s) value of 0.2 in order to maintain numerical stability. Another coefficient is the sub-grid scale turbulent Prandtl number (Pr_t), which is normally determined

by empirical correlations within the range of 0.2-0.9. Although dynamic procedures have been created for the modelling of these parameters, most fire simulations rely on constant values of Sc_t and Pr_t. In the particular case study both turbulent Pr_t and Sc_t values were chosen to be equal to 0.5. There are no rigorous justifications for these choices other than through direct comparison with experimental data for strong buoyant flows originating from enclosure fires occurring inside compartments. Turbulent vortices with a characteristic size larger than the filter width are calculated directly from the equations. As a result, it is possible to take into account the large-scale eddy formations in flames and investigate the dominant role of the developing buoyant forces. In such a mathematical formulation of eddy viscosity the dissipation of kinetic energy from the flow and the stabilization effect in the numerical algorithm can be effectively treated.

Thermal radiation is simulated using the finite volume methodology on the same grid as the flow solver. All solid surfaces are assigned thermal boundary conditions by taking into account information about the burning behaviour of the respective material. The time step is dynamically adjusted in order to satisfy the CFL criterion. The CFL condition asserts that the solution of the equations cannot be updated with a time step larger than that allowing a parcel of fluids to cross a grid cell. For most large-scale calculations where convective transport dominates diffusive, the CFL condition restricts the time step. The FDS code has undergone extensive validation studies [17, 19].

2.3 Simulation Details

FDS results are known to significantly depend on the size of the numerical grid due to LES approximation [20]. In the general context of compartment fire simulations, the quality of the utilized grid resolution is commonly assessed utilizing the non-dimensional $D^*/\delta x$ ratio, where D^* is a characteristic fire diameter and δx corresponds to the nominal size of the grid cell. The $D^*/\delta x$ ratio corresponds to the number of computational cells spanning D^* and is representative of the adequacy of the grid resolution. If the value of the $D^*/\delta x$ ratio is sufficiently large, the fire can be considered well resolved. Several studies have shown that values of 10 or more are required to adequately resolve most fires and obtain reliable flame temperatures [21, 22]. In the current study, aiming to fulfil the $D^*/\delta x > 10$ criterion and, at the same time, reduce the required computational cost, a 0.05 m cell size was selected.

In the current study, a constant 2070 kW heat release rate is used. The FDS code simulates combustion phenomena using a “mixture-fraction” model, assuming infinitely fast mixing of fuel and oxygen (fuel and oxygen cannot co-exist and they react at any temperature). The soot yield, which represents the fraction of n-heptane fuel mass converted to smoke particulates, is set equal to 1.5 %, according to available measurements [19]. The selected numerical grid consists of 8 computational meshes, thus allowing the utilization of the “parallel” version of the FDS code. The numerical grid extends to the outside of the enclosure, in order to effectively simulate air entrainment phenomena. The size of the physical domain “extensions”, 3.5 m in the x- and 2.5 m in the z-direction, have been selected following suggestions found in a relevant study on the effect of computational domain size on numerical simulation of compartment fires [23]. The total number of computational cells is 648.800 and the total simulation time is selected to be equal to 500 s. At the beginning of the numerical

simulation, the entire computational domain (both indoors and outdoors) is assumed to be still (zero velocity), exhibiting a temperature of 20^{o}C. Open boundaries are imposed at all boundaries external to the enclosure and wall boundary conditions are used at walls, ceiling and floor.

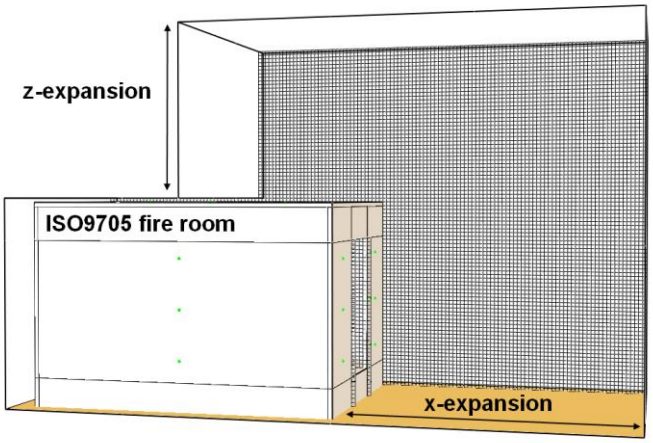

Figure 2. Physical domain and utilized computational mesh.

2.4 Parametric Study

Two test cases have been studied in order to investigate the impact of PCM addition on the fire characteristics of gypsum plasterboard; all simulation parameters are identical, except from the material used to construct the model room walls. In the first test case (GP), which served as a basis for comparison, 25 mm "conventional" gypsum plasterboards are used to clad the room walls. In the second test case (GP+PCM), paraffin-based PCM are assumed to be incorporated to the 25 mm gypsum plasterboards. The GP+PCM test case corresponds to "worst-case scenario" conditions, by assuming that all PCM encapsulation shells fail at high temperatures, thus allowing the entire quantity of PCM to be released in the fire region. Detailed temperature-dependent physical properties of gypsum plasterboards are used to describe their thermal behaviour.

3 FIRE BEHAVIOUR OF WALL ASSEMBLIES

Until now, there are no CFD simulations available in the open literature, focusing on the fire behaviour of PCM enriched gypsum plasterboard wall assemblies; however, there are few available studies that investigate the impact of the use of gypsum plasterboards as a building material under fire conditions [23, 24]. In order to improve the prediction quality in fire simulation studies, a detailed knowledge of the thermo-physical properties, associated with the behaviour of the respective building materials in high temperatures, is required. In this context, detailed measurements using both Differential Scanning Calorimetry (DSC) and Thermo Gravimetric Analysis (TGA) have been performed in order to determine the thermophysical behaviour of the different types of gypsum plasterboards at elevated temperatures and intense heating rates.

3.1 Gypsum Plasterboard

Gypsum plasterboards are widely used in the building industry for a variety of applications as an aesthetically pleasing, easily applied and mechanically enduring facing material for walls and ceilings. In the context of building fire safety, gypsum plasterboards are capable of decelerating the penetration of fire through walls and floors, due to the endothermic gypsum dehydration process occurring in high temperatures. When gypsum plasterboard is subjected to a high temperature environment, water molecules bound in its crystal lattice are released and transferred through the board, absorbing energy and thus reducing the mean wall temperature. This process is known to improve the fire resistance of the wall assembly, thus enhancing the safety margins of the building, by allowing longer evacuation times [24].

A typical gypsum plasterboard contains mainly gypsum, which consists mainly of calcium sulphate dihydrate ($CaSO_4 \cdot 2H_2O$), i.e. calcium sulphate di-hydrate with 21% (by weight) chemically bound water. When gypsum is heated above 90°C, the chemically bound water dissociates from the crystal lattice and evaporates. This process, known as gypsum "dehydration", occurs in the temperature region between 90°C and 250°C, depending on the heating rate; dehydration reactions are strongly endothermic, thus requiring large amounts of heat [25]. The dissociation of the chemical bound water takes place in two stages. In the first stage (Equation 1), the calcium sulphate dihydrate loses 75% of its water, thus forming calcium sulphate hemi-hydrate ($CaSO_4 \cdot \frac{1}{2}H_2O$). If the gypsum plasterboard is further heated, a second reaction occurs (Equation 2), where the calcium sulphate hemi-hydrate loses the remaining water to form calcium sulphate anhydrite ($CaSO_4$). Both reactions are highly endothermic.

$$CaSO_4 \cdot 2H_2O_{(s)} \rightarrow CaSO_4 \cdot {}^{1}/_{2}H_2O_{(s)} + {}^{3}/_{2}H_2O_{(g)} \quad (1)$$

$$CaSO_4 \cdot {}^{1}/_{2}H_2O_{(s)} \rightarrow CaSO_{4\,(s)} + {}^{1}/_{2}H_2O_{(g)} \quad (2)$$

The physical properties of gypsum vary with increasing temperature, due to the occurring dehydration reactions. The utilization of temperature-dependent physical properties is known to yield more accurate results in heat transfer simulations of gypsum plasterboards, compared to mean values [26] and therefore, temperature-dependent values for the thermal conductivity and specific heat were used in the simulations. The respective values have been obtained by using a 'CT-METRE' measuring device [27] and DSC analysis (Figure 3).

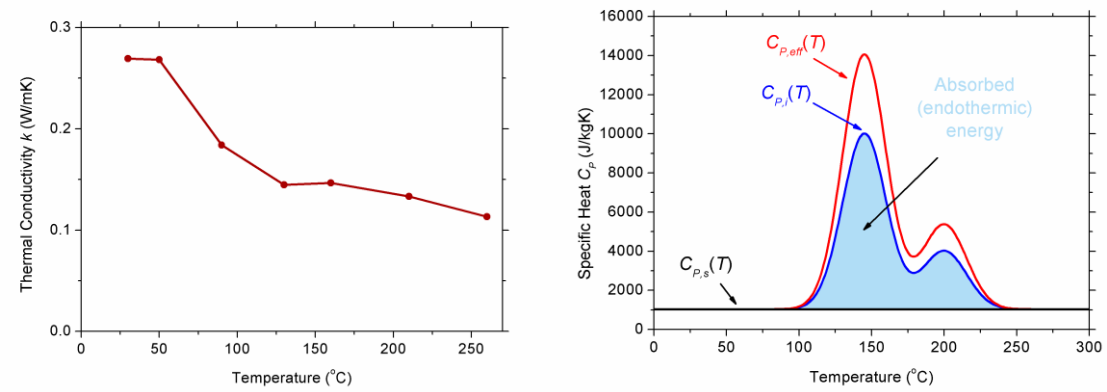

Figure 3. Temperature dependent thermo-physical properties of gypsum plasterboard.

Both gypsum dehydration and water vapour diffusion have a strong impact on the heat transfer characteristics of gypsum plasterboards exposed to fire conditions. In order to implement these effects in the utilized CFD code, a detailed solution of the respective heat and mass transfer equations across the width of the gypsum plasterboard would be required; since the computational cost of such simulations is currently prohibitive, an alternative methodology is followed. The effects of the aforementioned physical phenomena are incorporated into the specific heat, thus constructing an "effective" specific heat temperature profile, which is then utilized in the simulations. The effective specific heat of the gypsum plasterboards is determined using Equation (3). $C_{P,s}$ corresponds to the "true" specific heat of gypsum plasterboard, whereas the $C_{P,i}$ values correspond to the additional "effective" specific heat owed to the dehydration endothermic reactions occurring in elevated temperatures; the integral of each additional specific heat is equal to the energy absorbed in the respective reaction. The $C_{P,i}$ values have been estimated using DSC measurements of actual gypsum plasterboards. The f_i parameters correspond to mass transfer correction factors, which take into account the effects of vapour migration in the gypsum porous structure. The, in-house developed, HETRAN simulation tool [25], which simulates simultaneous heat and mass transfer in porous building materials, has been used to define the values of the mass transfer correction factors; their values were found to be approximately 1.45, corresponding to a 45% increase of the total dehydration energy. The temperature dependent "effective" specific heat values used in the simulations are depicted in Figure 3 (right).

$$C_{P,eff}(T) = C_{P,s}(T) + \sum_{i=1}^{N} f_i C_{P,i}(T) \tag{3}$$

3.2 Phase Change Materials

Aiming to investigate the thermal behaviour of commercial gypsum plasterboards enhanced with micro-encapsulated paraffin-based PCM, a series of DSC and TGA tests have been performed. Due to lack of information regarding the concentration of PCM, comparative TGA measurements in both a "plain" and "PCM-enhanced" gypsum plasterboard have been made, utilizing a relatively high heating rate (80^{o}C/min), pertaining to the "intense" fire environment. The obtained results (Figure 4) suggest that at temperatures higher than 300^{o}C, a significant mass loss, pertaining to approximately 21% of the initial mass of the commercially available PCM-enhanced gypsum plasterboard, is observed; it is assumed that this mass corresponds to the evaporating PCM.

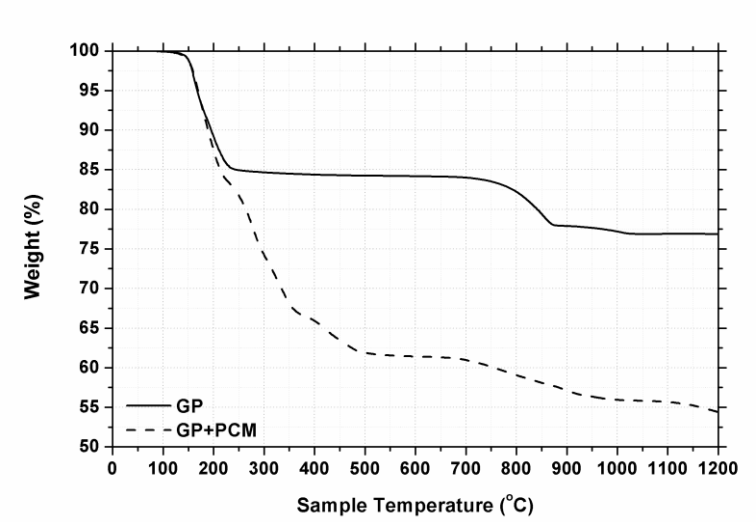

Figure 4. TGA curves of gypsum plasterboard with and without encapsulated PCM (80°C/min).

The temperature regions where phase change phenomena (solid-to-liquid and liquid-to-gas) occur have been determined by means of DSC analysis of the "pure" PCM, using an inert gas (nitrogen) atmosphere and two different heating rates, 0.5°C/min and 80°C/min (Table 1). In a fire environment, the observed heating rate can be as high as 1000°C/min [28]; as a result, intense heating rate value (80°C/min) has been utilized to identify the temperature region of PCM evaporation.

Heating Rate	Physical process	T_{onset} (°C)	T_{peak} (°C)	T_{endset} (°C)
0.5°C/min	PCM melting	25.88	27.33	27.88
80°C/min	PCM evaporation	260.78	294.96	311.48

Table 1: Phase change temperature ranges of the PCM blend (DSC measurements).

Measurements using the low heating rate (5°C/min) have been focused on the solid-to-liquid phase change process, aiming to identify the chemical composition of the paraffinic PCM blend. Commercially available paraffin-based PCM contain a large variety of paraffinic species, thus allowing better control of the overall thermal behaviour. The melting point of the PCM blend (27.33°C) has been found to correlate favourably to that of octadecane ($C_{18}H_{38}$, exhibiting a 27.85°C melting point). Therefore, in order to effectively simulate the fire behaviour of the PCM-enriched gypsum plasterboard, the PCM was assumed to consist entirely of octadecane. As a result, the main thermo-physical properties required for modelling purposes, such as latent heat of evaporation (207.11 kJ/kg) and lower heating value (43802.8 kJ/kg), were that of octadecane [29].

4 RESULTS AND DISCUSSION

4.1 Validation Study (GP Test Case)

It is well established that CFD codes can accurately predict thermal conditions and chemical species concentrations in over-ventilated single compartment fires, when experimental uncertainty is accounted for [30, 31]. In order to investigate the applicability and limitations

of the utilized numerical model, a preliminary validation study, using the GP test case, has been performed. Predictions have been compared to available experimental data [16]; however, since the experimental conditions have not been fully replicated in the simulations (e.g. utilization of a constant fire load instead of varying "steps", utilization of gypsum plasterboards as lining material instead of the ceramic fibre blanket used in the experiments), the obtained results are by no means intended to be considered as a validation study of the FDS code. Table 2 presents mean and standard deviation values of the experimentally measured and computed gas temperatures and volume concentrations of O_2, CO_2 and CO in Positions F and R (c.f. Figure 1). Predictions are found to exhibit a generally good quantitative agreement with the measurements. Gas temperatures are slightly under-predicted; this can be attributed to the fire not being fully developed in the utilized simulation time (500s) (c.f. Figure 7).

HRR = 2070kW	Position F				Position R			
	Experimental		Numerical		Experimental		Numerical	
	Mean	STD	Mean	STD	Mean	STD	Mean	STD
T_{gas} (^{o}C)	1163.49	31.97	912.11	45.83	1230.25	31.43	1067.37	67.30
O_2	0.04075	0.01005	0.03518	0.00845	0.03961	0.0106	0.05128	0.02307
CO_2	0.11596	0.00506	0.08562	0.00629	0.11191	0.00329	0.08007	0.01181
CO	0.00184	0.001288	0.00416	0.00337	0.005392	0.003661	0.00367	0.00488

Table 2: Average temperatures and volume fractions of major species at the front (Position F) and rear (Position R) sampling locations.

4.2 Characteristics of the Developing Flow-Field

Two characteristic time snapshots of the developing flow field and the respective predicted flame shape, 10s and 500s after fire initiation, are depicted in Figure 5. Both examined cases exhibit similar characteristics during the initial phase; however, paraffin vapour evaporation in case GP+PCM results in a significant enhancement of the fire intensity at the end of the simulation (500s), compared to the GP case. As expected, a typical thermal buoyant flow is established, thus generating a strong upward flow of the heated combustion products. The flame shape and location in the GP case is initially similar to a typical pool fire burning in the open environment; however, the growing recirculation zone, due to the air entrainment near the opening, leads to a slight deformation of the flame shape, which results in a "drift" towards the "rear" side of the enclosure. The required oxygen to sustain the combustion reactions is provided by air entrainment through the lower part of the opening. The effect of PCM vapour combustion is evident; the flame is clearly more intense, extending to a much larger volume in the GP+PCM case. Also, the buoyant upward flow of the hot plume rising beyond the opening is significantly enhanced; in addition, the recirculation region observed indoors is more intense compared to the GP case.

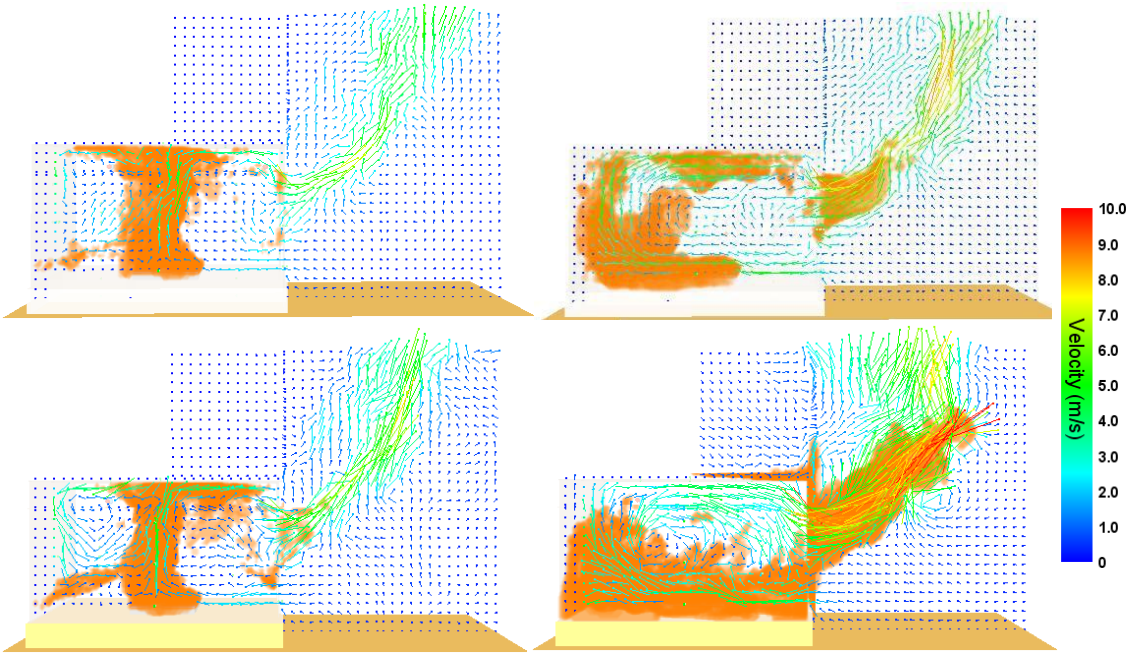

Figure 5. Predictions of gas mixture velocity and flame location, for test cases GP (top) and GP+PCM (bottom), 10s (left) and 500s (right) after fire initiation.

Predictions of the gas mixture temperature at the end of the simulation period for both the examined test cases are depicted in Figure 6. In the GP case, higher temperature values are observed inside the compartment, towards the rear end; however, the GP+PCM case results in a much broader and more intensified plume outside of the compartment. This effect is attributed to the increased fire load corresponding to the GP+PCM case, resulting in the development of significant external flaming conditions.

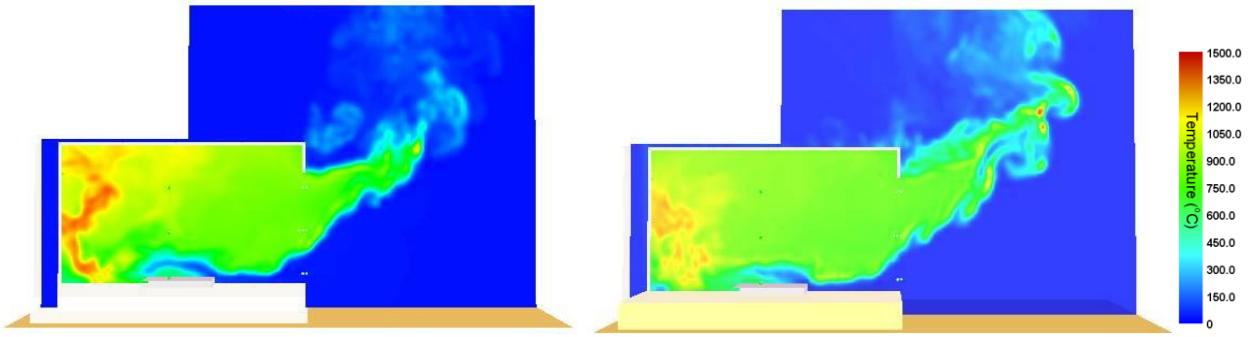

Figure 6. Predictions of gas mixture temperature 500 s after fire initiation, for test cases GP (left) and GP+PCM (right).

4.3 Thermal Effects of PCM

The global effect of PCM evaporation and subsequent combustion is evident in Figure 7, where predictions of the overall heat release rate (left) and burn rate (right) are depicted for both the examined test cases. Paraffin vapour combustion results in increasing the predicted burn rate by a factor of 3-6; however, these results should be considered indicative of the potential effect of PCM, since a "worst case scenario" has been assumed, where the entire mass of the PCM, which is initially micro-encapsulated in the gypsum plasterboards, is considered to evaporate and subsequently burn.

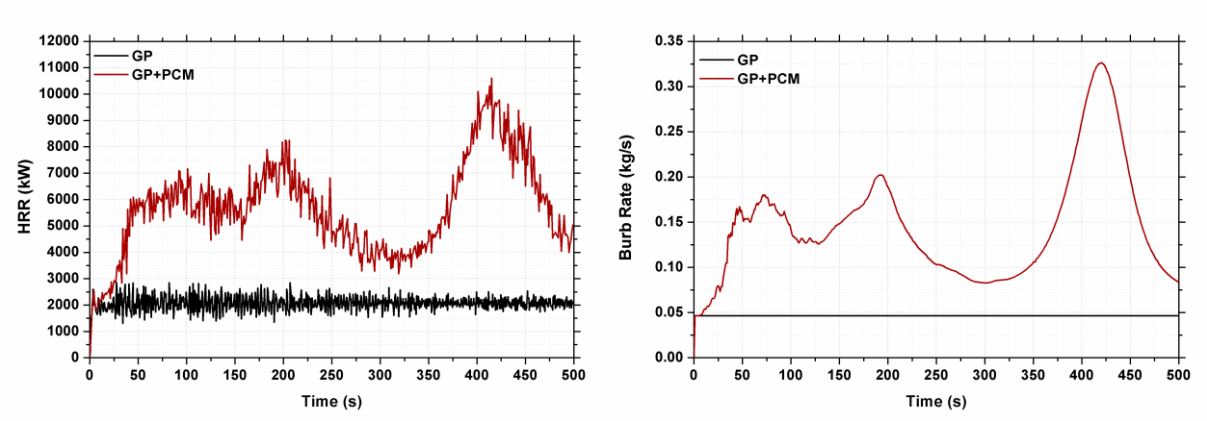

Figure 7. Predictions of heat release rate (left) and burn rate (right).

Predictions of the temporal evolution of the gas temperature, in Positions R (left) and F (right) are depicted in Figure 8. The observed oscillating behaviour is mainly attributed to the "puffing" phenomena commonly observed in pool fires. The puffing characteristics are mainly determined by the ambient air entrainment rate. Experimental evidence suggests that the puffing frequency is mainly dependent on the size of the pool and is almost unrelated to the fuel type [32]. The calculated puffing frequency in the GP case is approximately 1.5Hz; the time step used in the simulations, which varied between 2.2ms and 37ms in order to satisfy the CFL criterion, was adequately fine to capture this phenomenon.

It is evident that the gas temperatures near the opening (location F) are higher in the GP+PCM case, due to the additional fuel vapour produced by the PCM evaporation. However, close to the rear side of the compartment (location R), the GP case results in consistently higher temperatures; as it was mentioned before, this is attributed to the formation of an intense recirculation zone and the predominant movement of the hot gaseous products towards the rear side (c.f. Figure 5).

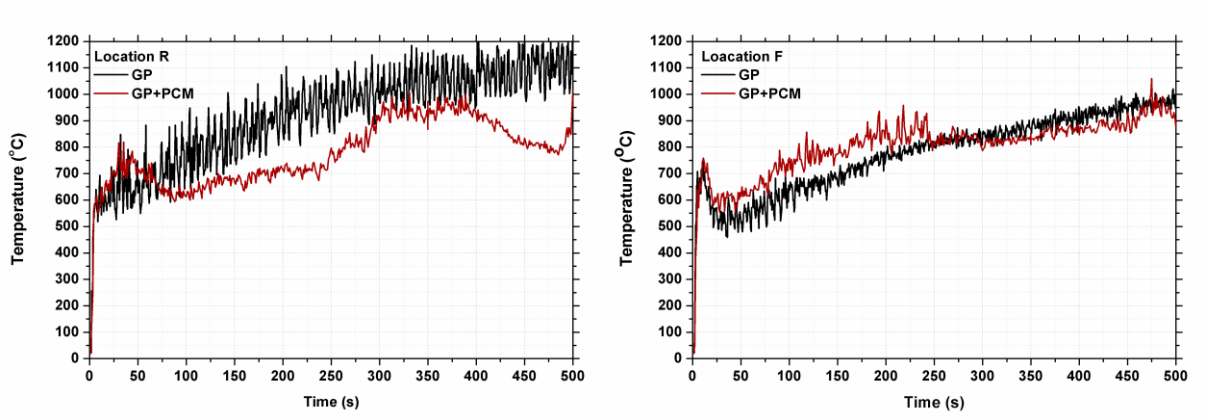

Figure 8. Predictions of the temporal evolution of gas temperatures at locations R (left) and F (right).

4.4 Wall Assembly Fire Resistance Characteristics

CFD tools allow the estimation of the fire resistance characteristics of the entire compartment and the constitutive building elements. In this context, the performed simulations are used to investigate the fire resistance of the utilized gypsum plasterboard wall assemblies. Gypsum plasterboards exposed to fire are considered to exhibit mechanical failure when cracks or openings are observed through the wall [33]; however, since cracking phenomena cannot be

accurately simulated in the FDS code, alternative failure criteria are used in this study.
According to the Eurocode standards [34], fire safety regulations regarding the integrity of a compartment wall assembly specify that the average temperature rise of the unexposed side of a building element should be limited to 140^{o}C and the maximum temperature rise to the unexposed side (ambient facing side) should not exceed 180^{o}C during the heating phase and until the maximum temperature in the fire compartment is reached. For the decay phase of the fire, the average temperature rise of the unexposed side should be limited to a temperature rise of 200^{o}C and not exceed 240^{o}C. In the current simulations, the ambient temperature was considered to be 20^{o}C; therefore, the aforementioned "failure" criterion for a gypsum plasterboard assembly corresponds to a temperature of 200^{o}C on its unexposed side.
Predictions of wall surface temperatures, across a section of the exposed side of Wall 2 and the unexposed side of Walls 4 and 5 (c.f. Figure 1), for both test cases are shown in Figure 9. Temperature predictions at the wall surfaces directly exposed to the fire are noticeably higher than the corresponding predictions at the unexposed side. As expected, the observed wall temperatures are generally higher in the case of PCM-enriched gypsum plasterboards; it is evident that the produced amount of "combustible" paraffin vapours enhances the fire power (c.f. Figure 7), thus resulting in higher wall temperatures.

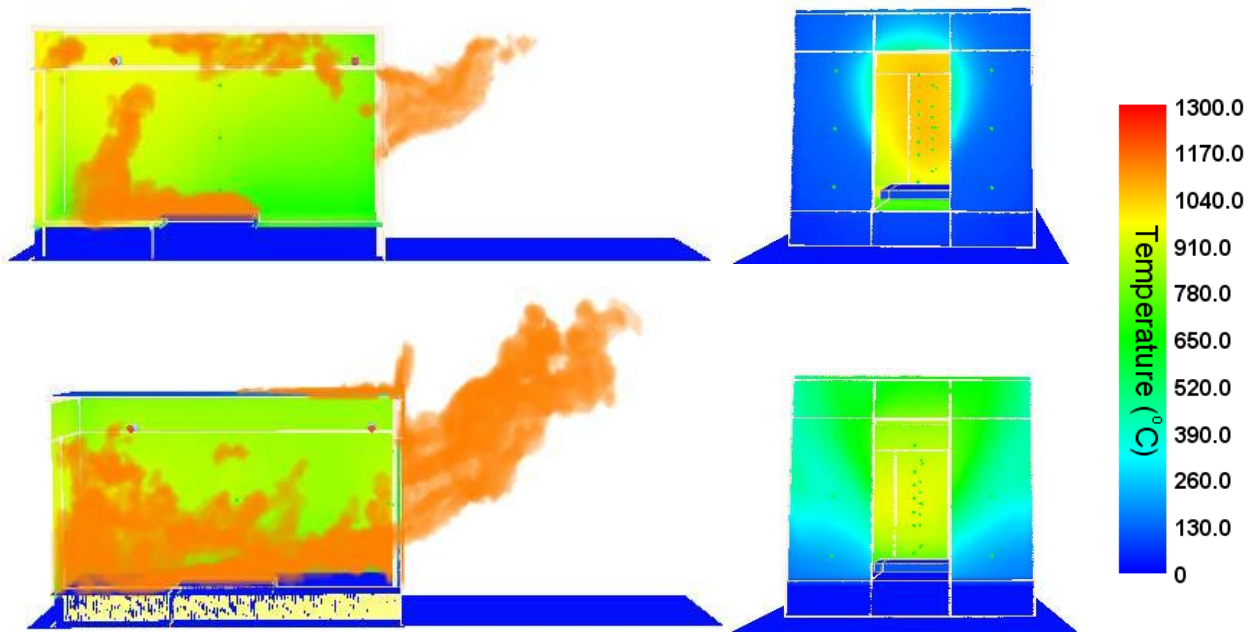

Figure 9. Predictions of exposed (left) and unexposed (right) wall surface temperatures and flame location 500s after fire initiation, for test cases GP (top) and GP+PCM (bottom).

Predictions of the temporal evolution of the exposed side temperatures for Walls 1 and 4 are depicted in Figure 10; the illustrated numerical results are obtained at a height of 1.2m. In both cases, the wall temperatures are rapidly increasing; however, the GP+PCM test case results in higher wall temperatures, especially in the case of Wall 4, which is adjacent to the opening of the compartment.

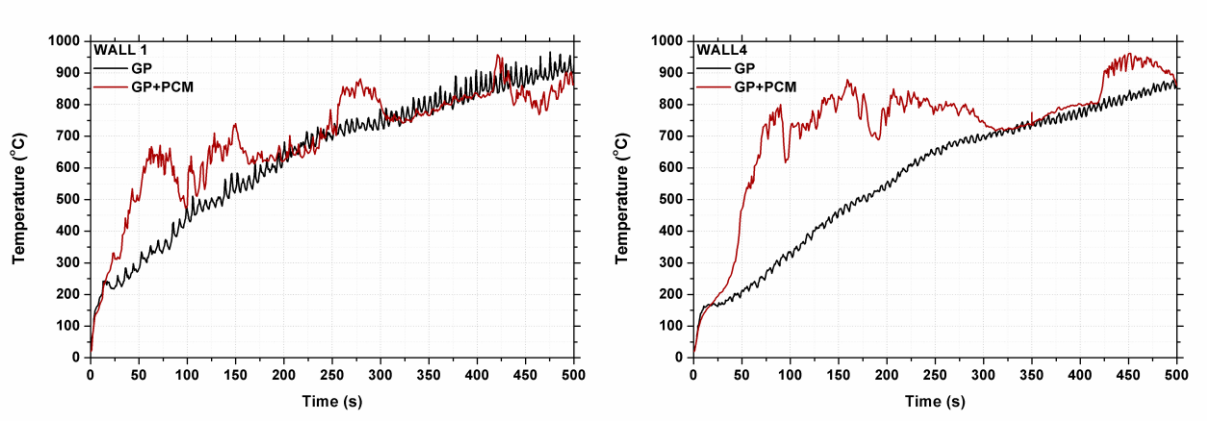

Figure 10. Predictions of the temporal evolution of the exposed surface temperature for Walls 1(left) and 4 (right), at a height of 1.2m.

Predictions of the temporal evolution of the unexposed surface temperature for Walls 1 and 4, at a height of 1.2 m. are depicted in Figure 11. It is evident that Wall 1 does not, in any case, exceed the Eurocode fire resistance "failure" criterion (temperature at the unexposed side higher than 200^{o}C). In the PCM enriched gypsum plasterboard case (GP+PCM), predicted temperatures of the unexposed side of Wall 4, which lies close to the opening, exceed the critical failure limit of 200^{o}C approximately 2 min after fire initiation. In the GP case, no "failure" event of the wall is observed.

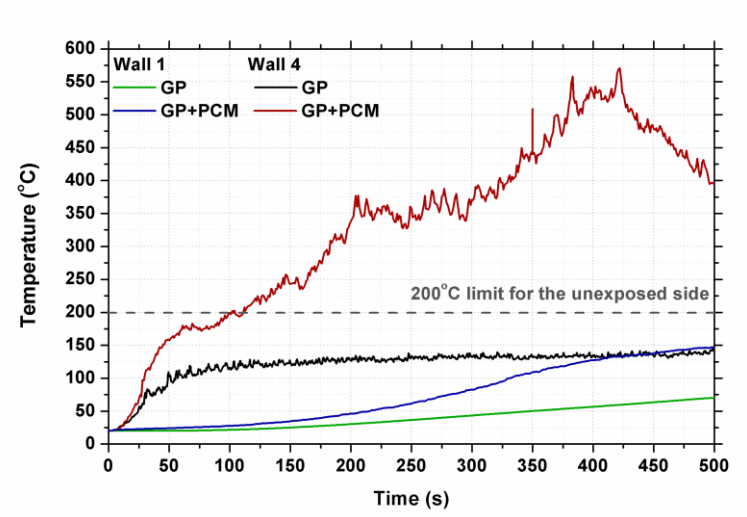

Figure 11. Predictions of the temporal evolution of the unexposed surface temperature for Walls 1 and 4, at a height of 1.2 m.

5 CONCLUSIONS

Thermal energy storage using PCM enhanced building materials provides significant advantages in terms of building energy consumption. In this context, there are already commercially available gypsum plasterboards which incorporate micro-encapsulated paraffin-based PCM; these innovative building materials posses various desirable characteristics, such as high heat of fusion, variable phase change temperature, no phase segregation and low cost,

but they may compromise the fire resistance characteristics of the building [8]. Aiming to investigate the effect of PCM addition in the fire resistance characteristics of gypsum plasterboards, a CFD study has been performed. In this frame, the FDS code has been used to simulate the flow- and thermal-fields developing in an ISO 9705 compartment during a fire event. The walls of the compartment were assumed to be constructed using two alternative drywall system configurations, one applying common gypsum plasterboards and the other using gypsum plasterboards enriched with paraffin-based PCM. Predictions of gas velocities, gas and wall temperatures revealed that, when the "PCM-enriched" gypsum plasterboards are exposed to a fire environment, paraffin vapours may be released to the main combustion area, thus enhancing the fire intensity and compromising fire resistance of the building elements. Further investigation is planned to be carried out on the different effects of incorporation methods, flame retardant addition in PCM blends used in gypsum plasterboards and application of non-flammable surface coatings.

6 AKNOWLEDGEMENTS

The present study has been financially supported by the E.C. in the frame of the FP7 projects "MESSIB: Multi-source Energy storage System Integrated in Buildings" (FP7-NMP-2007-LARGE-1) and "FC-DISTRICT: New m-CHP network technologies for energy efficient and sustainable districts" (Grant No. 260105).

REFERENCES

1. Quintiere, J.G., Fire behavior in building compartments, *Proceedings of the Combustion Institute*, **29**, 2002, pp. 181-193.
2. Merci, B. and Van Maele, K., Numerical simulation of full-scale enclosure fires in a small compartment with natural roof ventilation, *Fire Safety Journal*, **43**, 2008, pp. 495-511.
3. Olenick, S.M. and Carpenter, D., An updated international survey of computer models for fire and smoke, *Journal of Fire Protection Engineering*, **13**, 2003, pp. 611-666.
4. Makhviladze, G.M., Shamshin, A.V., Yakush, S.E. and Zykov, A.P., Experimental and numerical study of transient compartment fires, *Combustion, Explosion and Shock Waves*, **42**, 2006, pp. 723-730.
5. Wen, J.X., Kang, K., Donchev, T. and Karwatzki, J.M., Validation of FDS for the prediction of medium scale pool fires, *Fire Safety Journal*, **42**, 2007, pp. 127-138.
6. Agyenim, F., Hewitt, N., Eames, P. and Smyth, M., A review of materials, heat transfer and phase change problem formulation for latent heat thermal energy storage systems (LHTESS), *Renewable and Sustainable Energy Reviews*, **14**, 2010, pp. 615-628.
7. Voelker, C., Kornadt, O. and Ostry, M., Temperature reduction due to the application of phase change materials , *Energy and Buildings*, **40**, 2008, pp. 937-944.
8. Banu, D., Feldman D., Haghighat, F., Paris, J. and Hawes, D., Energy-storing wallbnoard: Flammability tests, Journal of Materials in Civil Engineering, **10**, No.2, 1998, pp. 98-105.
9. Zhou D., Zhao, C.Y. and Tina, Y., Review on thermal energy storage with phase change materials (PCMs) in building applications, *Applied Energy*, **92**, 2012, pp. 593-605.
10. Mandilaras, I. and Founti, M.A., Experimental investigation of agglomerate marbles containing phase change materials, Proceedings of the 11th International Conference on Thermal Energy Storage (Effstock), 14-17 June 2009, Stockholm, Sweden.
11. Hunger, M., Entrop, A.G., Mandilaras, I., Brouwers, H.J.H. and Founti, M., The behavior

of self-compacting concrete containing micro-encapsulated Phase Change Materials, *Cement and Concrete Composites*, **3**, 2009, pp. 731-743.
12. Hawlader, M.N.A., Uddin, M.S. and Khin, M.M., Microencapsulated PCM thermal-energy storage system, *Applied Energy*, **74**, 2003, pp. 195-202.
13. Sittisart, P. and Farid M.M, Fire retardants for phase change materials, Applied Energy, 88, 2011, pp. 3140-3145.
14. Cabeza, L.F., Castell, A., Barreneche, C., de Gracia, A. and Fernandez, A.I., Materials used as PCM in thermal energy storage in buildings: A review, Renewable and Sustainable Energy Reviews, 15, 2011, pp. 1675-1695.
15. Kosny, J., Yarbrough, D.W., Riazzi, T., Leuthold, D., Smith, J.B. and Bianchi, M., Development and testing of ignition resistant microencapsulated phase change material, Proceedings of the 11th International Congress on Thermal Energy Storage (Effstock), 14-17 June 2009, Stockholm, Sweden.
16. Lock, A., Bundy, M., Johnsson, E.L., Hamins, A., Ko, G.H., Hwang, C., Fuss, P. and Harris, R., Experimental study of the effects of fuel type, fuel distribution and vent size on full-scale underventilated compartment fires in an ISO 9705 room, NIST Technical Note 1603, National Institute of Standards and Technology, Gaithersburg, MD.
17. McGrattan, K., Hostikka, S. and Floyd, J., Fire Dynamics Simulator User's Guide, 2010.
18. Pope, S.B., Ten questions concerning the large eddy simulation of turbulent flows, *New Journal of Physics*, **6**, No. 35, 2004, pp.1-24.
19. McGrattan, K., Verification and validation of selected fire models for nuclear power plant applications, volume 7: Fire Dynamics Simulator (FDS), Final Report, NUREG-1824, EPRI 1011999.
20. Jahn, W., Rein, G., and Torero, J.L., A posteriori modelling of the growth phase of Dalmarnock Fire test One, *Building and environment*, **46**, 2011, pp. 1065-1073.
21. Lin, C.H., Ferng, Y.M. and Hsu, W.S., Investigating the effect of computational grid sizes on the predicted characteristics of thermal radiation for a fire, *Applied Thermal Engineering*, **29**, 2009, pp. 2243-2250.
22. McGrattan, K.B., Floyd, J., Forney, G., Baum, H. and Hostikka, S., In improved radiation and combustion routines for a large eddy simulation fire model, Proceedings of the 7th International Symposium of Fire Safety Science, Worcester, MA, 2002, pp. 827-838.
23. Zhang, X., Yang, M., Wang, J. and He, Y., Effects of computational domain on numerical simulation of building fires, *Journal of Fire Protection Engineering*, **20**, 2010, pp. 225-250.
24. Wang, C.Y. and Ang, C.N., Effect of moisture transfer on specific heat of gypsum plasterboard at high tempratures, *Construction and Building Material*, **16**, 2004, pp. 505-515.
25. Kontogeorgos, D.A. and Founti, M.A., Numerical investigation of simultaneous heat and mass transfer mechanisms occurring in a gypsumboard exposed to fire, *Applied Thermal Engineering*, **30**, 2010, pp. 1461-1469.
26. Kontogeorgos, D.A., Kolaitis, D.I. and Founti, M.A., Numerical modelling of heat transfer in gypsum plasterboards exposed to fire, Proceedings of the 6th International Conference on Heat Transfer, Fluid Mechanics and Thermodynamics, 11-13 July 2008, Pretoria, South Africa.
27. Kontogeorgos, K., Mandilaras, I. and Founti, M., Scrutinizing gypsum board thermal performance at dehydration temperatures, *Journal of Fire Sciences*, **29**, 2011, pp. 111-130.
28. Matala, A., Lautenberger, C. and Hostikka, S., Generalized direct method for Pyrolysis kinetic parameter estimation and comparison to existing methods, *Journal of Fire Sciences*, **30,** No. 4, 2012, pp.339-356.

29. Yaws, C.L., Handbook of Thermodynamic and Physical Properties of Chemical Compounds, 1996, electronic edition. Knovel, Norwich, NY (update *2004*).
30. Hamins, A., Johnsson, E., Donnelly, M. and Maranghides, A., Energy balance in a large compartment fire, *Fire Safety Journal*, **43**, 2008, pp. 180-188.
31. Pierce, J.B.M. and Moss, J.B., Smoke production, radiation heat transfer and fire growth in a liquid-fuelled compartment fire, *Fire Safety Journal*, **42**, 2007, pp. 310-320.
32. Ghoniem, A.F., Lakkis, I. and Soteriou, M., Numerical simulation of the dynamics of large fire plumes and the phenomenon of puffing, 26th Symp. (Int.) on Combustion, The Combustion Inst., 1996, pp. 1531-1539.
33. Manzello, L.S., Gann, G.R., Kukuck, R.S. and Lenhert, B.D., Influence of gypsum board type on real fire performance of partition assemblies, *Fire and Materials*, **31**, 2007, pp. 425-442.
34. EN 1992-1-2, Eurocode 2, Design of concrete structures – Part 1-2: General rules – Structural fire design. 2004.